Hemodynamic Aspects of Mitral Regurgitation Assessed by Generalized Phase-Contrast Magnetic Resonance Imaging

Petter Dyverfeldt, John-Peder Escobar Kvitting, Carl Johan Carlhäll, Gabriella Boano, Andreas Sigfridsson, Ulf Hermansson, Ann F. Bolger, Jan Engvall and Tino Ebbers

Hemodynamic Aspects of Mitral Regurgitation Assessed by Generalized Phase-Contrast Magnetic Resonance Imaging

Petter Dyverfeldt (PhD)[1,2,3], John-Peder Escobar Kvitting (MD, PhD)[3,4], Carl Johan Carlhäll (MD, PhD)[3,5], Gabriella Boano (MD)[4], Andreas Sigfridsson (PhD)[1,3,6], Ulf Hermansson (MD)[4], Ann F. Bolger (MD)[1,7], Jan Engvall (MD, PhD)[1], Tino Ebbers (PhD)[1,2,3]

[1]Division of Cardiovascular Medicine, Department of Medical and Health Sciences, Linköping University, Linköping, Sweden.

[2]Division of Applied Thermodynamics and Fluid Mechanics, Department of Management and Engineering, Linköping University, Linköping, Sweden.

[3]Center for Medical Image Science and Visualization (CMIV), Linköping University, Linköping, Sweden.

[4]Department of Cardiothoracic Surgery, Linköping University Hospital, Linköping, Sweden.

[5]Department of Clinical Physiology, Linköping University Hospital, Linköping, Sweden.

[6]Division of Medical Informatics, Department of Biomedical Engineering, Linköping University, Linköping, Sweden.

[7]Department of Medicine, University of California San Francisco, San Francisco, California, United States.

Correspondence: Petter Dyverfeldt, Linköping University,
Dept. of Medical and Health Sciences, Div. of Cardiovascular Medicine,
SE-581 83 Linköping, Sweden.
E-mail: petter.dyverfeldt@liu.se

Presented in part at the 17th ISMRM Scientific Meeting in Honolulu, HI, United States and at the ISMRM Workshop on Cardiovascular Flow, Function and Tissue Mechanics in Sintra, Portugal, 2009.

Grant Sponsors: Swedish Research Council, Swedish Heart-Lung Foundation, Heart Foundation at Linköping University.

Running Title: Hemodynamics of Mitral Regurgitation

ABSTRACT

Purpose: To investigate the utility of MRI measurement of left atrial (LA) flow patterns and turbulent kinetic energy (TKE) in patients with clinically significant mitral regurgitation.

Materials and Methods: Three-dimensional cine phase-contrast MRI (PC-MRI) data were acquired in five patients with posterior mitral leaflet prolapse and two normal volunteers. LA flow patterns were assessed using particle trace visualization. Specifically, vortices were recognized by closed streamlines. LA flow distortion was assessed by estimation of TKE. In addition, the regurgitant volume was measured.

Results: Four of the mitral regurgitation patients had eccentric regurgitant jets directed towards the septum; one patient had a central jet. The dominant systolic vortex was located in proximity to the regurgitant jet. The LA flow was highly disturbed with elevated values of TKE; peak LA TKE ranged from 13 to 37 millijoule and occurred consistently at late systole. The average LA TKE per cardiac cycle was significantly related to the regurgitant volume (TKE = 0.573 + 0.179·RegVol, $R^2 = 0.983$).

Conclusion: MRI permits investigations of atrial flow patterns and TKE in significant mitral regurgitation. The degree of LA flow distortion, as measured by the average LA TKE over one cardiac cycle, appears to reflect the severity of regurgitation.

Key Words: Hemodynamics, mitral valve insufficiency, turbulent flow, phase-contrast magnetic resonance imaging, pulmonary veins, blood flow velocity.

INTRODUCTION

Mitral valve regurgitation is a common valve lesion associated with progressive left atrial (LA) and left ventricular (LV) remodelling (1). Abnormal blood flow is both a consequence and pivotal driver of this process. The high-speed mitral regurgitant jet contributes both pressure and volume to the LA, and can cause flow reversal in the pulmonary veins and highly disturbed or even turbulent atrial flow. Fluid mechanical forces in disturbed and turbulent flows can damage blood constituents and surrounding tissue and have been implicated in increased risk of red blood cell damage (2) and platelet activation (3). Additionally, turbulence is the major cause of pressure drop in cardiovascular blood flow.

Clinically, echocardiography is the method of choice for assessment of mitral valve regurgitation. Two-dimensional trans-thoracic echocardiography can measure the size and function of the LA and LV. In addition, echo Doppler can provide useful information on regurgitant jet timing and distribution, regurgitant volume, effective regurgitant orifice area and pulmonary venous inflow (4). Transesophageal or three-dimensional (3D) echocardiography yield more accurate descriptions of the anatomical lesion underlying the regurgitation (5).

Magnetic resonance imaging (MRI) has several applications in mitral regurgitation, including functional assessment based on morphological cine images, quantification of ventricular size and mass, and measurement of regurgitant volume and fraction (6-8). The regurgitant fraction obtained with MRI can be converted into a qualitative grading of severity with good correlation to echocardiography (9). Other MRI techniques permit direct measurement of regurgitant volumes (10,11), estimation of peak velocities in flow jets (12), and flow pattern analysis of the time-varying three-dimensional (3D) LA blood flow (13). It is well known that the disturbed LA

flow that results from the regurgitant jet can cause signal loss in images acquired with gradient-echo or balanced steady state free-precession (bSSFP) sequences. This has been exploited in order to assess the severity of regurgitation (14,15). However, the utility of semi-quantitative hemodynamic evaluation based on signal loss alone is limited as variation in imaging parameters will greatly affect the extent and degree of the signal loss (16).

Disturbed and turbulent flows are characterized by velocity fluctuations. The fluctuation of velocity in an arbitrary direction, i, is defined by $u_i' = u_i - U_i$, where u_i is the velocity and U_i is the mean velocity as obtained by time, space, or ensemble averaging. The intensity of the velocity fluctuations (turbulence intensity) can be measured in different directions by the standard deviation, $\sqrt{\overline{u_i'^2}}$ (17). Using MRI, the turbulence intensity can be quantified by exploiting the effects of velocity fluctuations on the MRI signal magnitude (18-21). While conventional fluid dynamics methods, such as laser Doppler and thermal anemometry, utilize time averaging to sample the velocity fluctuations, the sampling of velocity fluctuations in MRI is spatial in the sense that the individual velocity of each spin within a voxel contributes to the MRI signal (22). In addition to the sampling obtained by the spatial extent of the voxel, the temporal sampling during the buildup of k-space assists in sampling the larger turbulence scales (22). Recent investigations have demonstrated good agreement between MRI measurements of turbulence intensity and large eddy simulations (22) as well as particle image velocimetry (23). They have also demonstrated that flow phenomena other than velocity fluctuations, such as spatial mean velocity gradients, appear to have negligible effects on MRI measurements of turbulence intensity (22). The capability of MRI measurements of turbulence intensity to provide valuable information regarding disturbed flows has been documented both in-vitro (23) and in-vivo (24).

The aim of this study was to investigate the utility of MRI measurement of turbulence intensity and LA flow patterns in patients with clinically significant mitral regurgitation.

MATERIALS AND METHODS

Study Population

Seven subjects were included (table 1): five patients (Pat1-5) scheduled for mitral valve repair due to prolapse of the middle scallop of the posterior mitral leaflet, and two normal subjects (N1-2). The study was approved by the regional ethical review board and written informed consent was obtained from all participants. All subjects had undergone an echocardiography examination (table 1) up to four weeks prior to the MRI examination and the patients subsequently underwent mitral valve repair within three days. The intraoperative details of the mitral valve morphology are described in table 2.

MRI Measurements and Data Processing

MRI measurements were made using a clinical 1.5 T scanner (Phillips Achieva, Phillips Healthcare, Best, the Netherlands). Cardiac cine bSSFP imaging was applied to acquire long-axis images and a stack of short-axis images in 30 time frames. The short-axis images were acquired with a pixel size of 1.4x1.4 mm^2, slice thickness of 8 mm. 2D cine through-plane phase-contrast (PC) MRI (Patients: pixel size 1.6x1.6 mm^2, slice thickness 4 mm, temporal resolution 26 ms, TE/TR 4.0/6.6 ms, VENC = 4 m/s; Normal subjects: pixel size 1.6x1.6 mm^2, slice thickness 7 mm, temporal resolution 26 ms, TE/TR 3.0/5.0 ms, VENC = 2 m/s) was applied to measure the outflow from the LV to the aorta.

Generalized 3D cine PC-MRI was used to acquire data for the determination of flow patterns and turbulence intensity (24). The 3D cine PC-MRI data were acquired during free-breathing using a navigator-gated RF-spoiled gradient-echo pulse sequence with interleaved three-directional motion encoding. The peak velocities of the regurgitant flow measured with continuous wave echo Doppler were approximately 6 m/s (table 1). In order to achieve adequate dynamic range in the turbulence intensity estimation and velocity-to-noise ratio at other intracardiac regions, the PC-MRI velocity encoding range (VENC) parameter was set to 1.5 m/s, sacrificing the high velocities in the regurgitant jet. In the normal subjects without mitral regurgitation, a VENC of 100 cm/s was used. Imaging parameters included: TR 5.9-6.5 ms, TE 3.4-3.7 ms, flip angle 8°, SENSE reduction factor 2, voxel size 3x3x3 mm^3. The field-of-view and matrix size were adjusted to fit each specific subject. Two *k*-space lines in each flow-encoding segment were acquired per cardiac cycle, resulting in a temporal resolution of about 50 ms. Respiration effects were minimized by using navigator gating with a window size of 5 mm and 10 mm in the inner 25% and the outer 75% of the *k*-space, respectively. Scan time, excluding the navigator gating efficiency, was 10-15 minutes. The navigator gating efficiency was around 50%.

The interleaved 3D cine PC-MRI data were reconstructed into 40 time frames using a temporal sliding-window approach on the MRI scanner (Philips Healthcare, Best, the Netherlands). The velocity data were corrected on the scanner for concomitant gradient field effects. Corrections for background phase-errors were made in automated offline post-processing using a fourth-order weighted background-correction scheme (25). Generalized PC-MRI permits the reconstruction of mean velocity and turbulence intensity images from the data acquired in a single PC-MRI scan (21). The mean velocity is computed by conventional phase-subtraction (26) and the turbulence intensity is obtained from the magnitude ratio of two PC-MRI flow encoding segments acquired

with different first gradient moments. The turbulence intensity is obtained based on the assumption that the intravoxel velocity distribution is Gaussian, which implies that the MR signal magnitude as a function of applied motion sensitivity will be Gaussian as well. The relationship between the standard deviation of the intravoxel velocity distribution, σ, and two measurements of the MRI signal, $S(k_v)$ is (19,21):

$$\sigma = \mathrm{sqrt}\left[\frac{2\ln\left(\left|S\left(k_{v_2}\right)\right| / \left|S\left(k_{v_1}\right)\right|\right)}{k_{v_1}^2 - k_{v_2}^2}\right], \left|k_{v_1}\right| \neq \left|k_{v_2}\right| \qquad \text{[Eq. 1]}$$

where k_v is the applied motion sensitivity as obtained by taking the product between the gyromagnetic ratio and the 1st moment of the applied gradient waveform. In this way, the mean velocity and the turbulence intensity was computed from the single 3D cine PC-MRI dataset acquired in each subject. This was done in each voxel in each timeframe. Based on the turbulence intensity (intensity of the velocity fluctuations, $\overline{u_i'^2}$) in three directions, the turbulent kinetic energy (TKE) per unit volume was computed according to: TKE = $\frac{1}{2}\rho\sum_{i=1}^{3}\overline{u_i'^2}$ [J m^{-3}], where ρ is the density of blood (17,24). The TKE is a direction-independent measure of turbulence intensity.

Data Analysis

The MRI data were written to a file-format compatible with commercially available visualization software (EnSight 8.2, CEI Inc., Apex, NC, US). Using EnSight, the global flow velocity patterns in the LA were assessed using streamlines and pathlines visualization. Specifically, vortices were recognized by apparently closed streamlines detected by visual inspection. Vortex analysis was performed in the region of LA inflow from the left pulmonary veins to identify vortices which have previously been documented in normal subjects (13). Visualization of the spatial and

temporal distribution of elevated turbulence intensity was achieved by iso-surface rendering of the TKE in the LA.

To obtain a measure of the total extent of LA flow distortion created by the regurgitation, the TKE was integrated over the entire LA volume for all time frames of the cardiac cycle. Geometrical constraints were defined by manual segmentation of the LA, by which other regions that may potentially contain elevated TKE values (such as the ascending aorta) were specifically excluded. The average LA TKE per cardiac cycle was computed as the sum of the total LA TKE for all time frames divided by the number of time frames.

The regurgitant volume was computed by subtraction of the ascending aortic flow volume from the LV stroke volume. The aortic flow volume was computed from the 2D through-plane PC-MRI velocity measurement and the LV stroke volume was obtained by short-axis planimetry at end-systole and end-diastole. The necessary segmentations of the aorta and the LV were made manually, using freely available software (Segment v1.8; http://segment.heiberg.se) (27). We used simple linear regression with regurgitant volume as the independent variable and average TKE per cardiac cycle as dependent to assess the relationship between regurgitant volume and TKE. The model could not be significantly improved by adding squared regurgitant volume or using separate lines for patients and normal subjects.

Klein and colleagues (28), among others, have reported that the time-velocity profiles of inflow may differ between pulmonary veins in patients with mitral regurgitation. To investigate this we utilized the ability of 3D cine PC-MRI to make simultaneous velocity measurements in all pulmonary veins. From the 3D cine PC-MRI velocity data, the velocity in the principal flow

direction in the center of each vein close to its orifice was plotted over time. The variance between the individual pulmonary vein velocities was computed in each time frame over the complete cardiac cycle, providing a measure of the degree of discordance among the individual pulmonary veins' inflow.

RESULTS

The echocardiography data, summarized in table 1, indicated that the LV size of Patient 2 was at the upper limit of the normal range and the other patients were above the normal range.

As expected with the VENC set to 150 cm/s the 3D cine PC-MRI velocity data in the high-speed regurgitant jet were severely aliased and as a result the jet was not well visualized. Based on ultrasound and the available MRI data, four of the patients (Patients 2-5) had eccentric regurgitant jets directed towards the interatrial septum. One patient with more limited prolapse of only a discrete portion of the middle scallop of the posterior leaflet (Patient 1) had a more central jet. In the normal subjects, a distinct vortex developed near the inflow from the left pulmonary veins during both systole and diastole (figure 1). That vortex was diminished in the patients. Instead, the dominant systolic vortex in the patients occurred near the route of the regurgitant jet along the atrial septum (figure 1).

Visualizations of the TKE data demonstrated elevated turbulence intensity along the course of the regurgitant flow in all patients, as exemplified in figure 2 and movie 1. While the direction of the regurgitant jet naturally provides information on where to expect disturbed LA flow, the spatial distribution of TKE was highly three-dimensional. In the patients with eccentric jets directed towards the interatrial septum, regions of flow with high TKE extended anteriorly and posteriorly

over the septum. For each subject, the temporal evolution of the total TKE in the LA is shown in figure 3. In the patients, the total TKE consistently reached its maximum in late systole (at about 35% of the RR-interval), when the velocities of the regurgitation jet were declining. Peak total LA TKE ranged from 13 to 37 mJ. The regurgitant volume in the patients ranged from 31 to 81 ml; a plot of the regurgitant volume versus the average TKE in the LA per cardiac cycle is shown in figure 4. The estimated regression function was TKE = 0.573 + 0.179 RegVol, $R^2 = 0.983$. The intercept was not significantly different from zero. The slope was significantly different from zero, $p < 0.001$.

Based on the time-velocity profiles in the pulmonary veins obtained from the 3D cine PC-MRI velocity data, the pulmonary venous flow in the normal subjects had a higher peak velocity in systole compared to diastole, as expected at their ages. This systolic dominance was reversed in the patients with largest regurgitant volumes. Pronounced discordances in late systolic velocity values among different pulmonary veins were observed in three of the patients (Patients 2-4). This is shown in figure 5, where the variance (discordance) of the velocities in the different pulmonary veins is plotted over time for each subject. The time point at which these discordances are greatest corresponds to the time point at which the total TKE, shown in figure 3, reached its peak. In the patients with the smallest (Patient 1) and largest (Patient 5) regurgitant volume and TKE, no large velocity discordances were seen between the pulmonary veins at this time point.

DISCUSSION

In this study, generalized PC-MRI was used to investigate flow patterns and turbulence intensity in the LA of patients with clinically significant mitral regurgitation due to posterior leaflet prolapse. In all patients, the high momentum regurgitant jet caused disturbed LA flow with

elevated values of TKE; peak LA TKE occurred consistently at late systole. The LA TKE per heart beat was significantly related to the regurgitant volume. LA flow patterns were impacted by the regurgitant jet; the normal systolic LA vortex was diminished and a pronounced vortical flow appeared near the regurgitant jet. An approach to the quantification of discordant flow in the pulmonary veins was outlined; in the present study, discordant flow could not be related to global LA flow parameters or the direction of the regurgitant jet.

The close relation between LA TKE per cardiac cycle and regurgitant volume suggests that this quantitative measure of flow distortion reflects the severity of regurgitation (figure 4). Recent investigations have shown that the regurgitant volume correlates with the anatomic orifice area (29) in both mitral regurgitation and aortic regurgitation (30). In patients with mitral regurgitation, the anatomic mitral regurgitant orifice area agrees closely with the effective regurgitant orifice area estimated with clinical echocardiographic proximal isovelocity surface area (PISA) methods (31). Considering these relationships, hemodynamic effects of the regurgitation, such as the flow disturbances reflected by elevated values of TKE, might contribute to the correlation between measures such as the effective regurgitant orifice area and the clinical outcome of patients with asymptomatic mitral regurgitation (32). TKE measurements could add new perspectives in gauging the severity of mitral regurgitation.

In terms of LA flow patterns, a previous investigation has shown that a distinct vortex develops near the inflow from the left pulmonary veins during both systole and diastole in normal subjects (13); this was confirmed in the normal subjects of our present study as well. In the patients, the global LA flow was altered by the high-momentum regurgitant jet, with the appearance of a dominant systolic vortex near the interatrial septum and regurgitant jet (figure 1). Whether these

flow patterns would be similar in cases of eccentric mitral regurgitation jets directed towards the lateral wall instead of the septum is an intriguing question for future studies.

Because of the elevation in LA pressure that results from the regurgitant flow volume, blunted or reversed pulmonary venous flow can often be observed during systole in patients with significant mitral regurgitation (33). It has also been reported that there can be pronounced differences between the different veins (28). In the present study, this difference was quantified by computing the variance between the simultaneously recorded velocity-time profiles in each subject (figure 5). This computation was based on both right sided pulmonary veins and one or two left sided veins; separate outlets of the two left sided veins could not be detected in all subjects. In three of the patients (Patients 2-4) pronounced variance was identified between the velocities in the different pulmonary veins at end-systole (figure 5), when the pulmonary flow in general is either blunted or reversed. However, the patient with the largest regurgitant volume and the highest total TKE (Patient 5) demonstrated low systolic variance. Note that all these patients (Patients 2-5) had eccentric jets directed towards the atrial septum. In agreement with previous studies (28,34,35), these findings indicate that neither jet direction nor global flow parameters such as regurgitant volume and total TKE are sufficient to predict pulmonary venous flow discordances. One factor that may assist in explaining the differences in the time-velocity profiles between different pulmonary veins is the fact that the highly disturbed flow in the LA of these patients, manifested by elevated values of TKE, gives rise to local LA pressure differences. In this way, each pulmonary venous inflow may face a different atrial pressure.

Organic mitral regurgitation is a diverse disease secondary to structural alterations of the valvular apparatus. The present results are based on a sample of patients with posterior mitral leaflet

prolapse (table 2). Further studies in a larger number of patients with different mitral valve lesions may extend the present findings to a broader context and would permit evaluations of the clinical utility of TKE measurements. The growing referral of asymptomatic patients with mitral regurgitation to reconstructive valve surgery has led to an increasing demand for quantitative non-invasive tools to identify patients who would benefit from early surgical management. MRI determination of flow patterns and turbulence intensity add a new, quantitative dimension to the evaluation of disturbed cardiovascular hemodynamics and may provide novel perspectives on risk stratification of patients with regurgitant valve disease.

Study Limitations

There are several limitations to be addressed with regard to the present study. In terms of the vortical flow analysis, details regarding the extent and timing of the vortex in proximity to the regurgitant jet were not analyzed; reliable quantification of these parameters would require higher spatiotemporal resolution and increased dynamic range than provided by the imaging protocol used. The analysis of pulmonary venous velocities was based on the velocity of a voxel in the center of the lumen, rather that in a plane of voxels covering the entire lumen. In the case of complex velocity profiles, this will lead to inaccurate velocity estimations. Another limitation is the small number of normal volunteers included; no statistical comparison can be made between normal volunteers and patients. However, the findings in the normal volunteers are supported by previous investigations of vortex formation (13) and pulmonary venous velocities (36). In addition, the LA TKE can be expected to be low in any normal subject.

In conclusion, generalized PC-MRI permits investigations of atrial flow patterns and TKE in significant mitral regurgitation, and demonstrates the impact of the highly disturbed blood flow in

the LA. The degree of LA flow distortion, as measured by the average LA TKE over one cardiac cycle, appears to reflect the severity of regurgitation.

ACKNOWLEDGEMENT

The authors thank XXX for assistance with MRI data acquisition and XXX for assistance with statistical analysis. Grant support is acknowledged from XXX.

REFERENCES

1. Delahaye J, Gare J, Viguier E, Delahaye F, De Gevigney G, Milon H. Natural history of severe mitral regurgitation. Eur Heart J 1991;12(suppl B):5-9.
2. Sallam AM, Hwang NH. Human red blood cell hemolysis in a turbulent shear flow: contribution of Reynolds shear stresses. Biorheology 1984;21(6):783-797.
3. Stein PD, Sabbah HN. Measured turbulence and its effect on thrombus formation. Circulation Research 1974;35(4):608-614.
4. Patel AR, Mochizuki Y, Yao J, Pandian NG. Mitral regurgitation: comprehensive assessment by echocardiography. Echocardiography 2000;17(3):275-283.
5. Salustri A, Becker AE, van Herwerden L, Vletter WB, Ten Cate FJ, Roelandt JRTC. Three-dimensional echocardiography of normal and pathologic mitral valve: a comparison with two-dimensional transesophageal echocardiography. Journal of the American College of Cardiology 1996;27(6):1502-1510.
6. Ordovás KG, Reddy GP, Higgins CB. MRI in nonischemic acquired heart disease. J Magn Reson Imaging 2008;27(6):1195-1213.
7. Cawley P, Maki J, Otto C. Cardiovascular Magnetic Resonance Imaging for Valvular Heart Disease: Technique and Validation. Circulation 2009;119(3):468.
8. Chan K, Wage R, Symmonds K, Rahman-Haley S, Mohiaddin R, Firmin D, Pepper J, Pennell D, Kilner P. Towards comprehensive assessment of mitral regurgitation using cardiovascular magnetic resonance. Journal of Cardiovascular Magnetic Resonance 2008;10(1):61.
9. Gelfand EV, Hughes S, Hauser TH, Yeon SB, Goepfert L, Kissinger KV, Rofsky NM, Manning WJ. Severity of mitral and aortic regurgitation as assessed by cardiovascular magnetic resonance: optimizing correlation with Doppler echocardiography. Journal of Cardiovascular Magnetic Resonance 2006;8(3):503-507.
10. Kozerke S, Schwitter J, Pedersen E, Boesiger P. Aortic and mitral regurgitation: Quantification using moving slice velocity mapping. Journal of Magnetic Resonance Imaging 2001;14(2):106-112.
11. Westenberg J, Danilouchkine M, Doornbos J, Bax J, van der Geest R, Labadie G, Lamb H, Versteegh M, de Roos A, Reiber J. Accurate and Reproducible Mitral Valvular Blood

Flow Measurement with Three-Directional Velocity-Encoded Magnetic Resonance Imaging. Journal of Cardiovascular Magnetic Resonance 2004;6(4):767-776.

12. Nayak KS, Hu BS, Nishimura DG. Rapid quantitation of high-speed flow jets. Magnetic Resonance in Medicine 2003;50(2):366-372.
13. Fyrenius A, Wigström L, Ebbers T, Karlsson M, Engvall J, Bolger AF. Three dimensional flow in the human left atrium. Heart 2001;86(4):448-455.
14. Sechtem U, Pflugfelder PW, Cassidy MM, White RD, Cheitlin MD, Schiller NB, Higgins CB. Mitral or aortic regurgitation: quantification of regurgitant volumes with cine MR imaging. Radiology 1988;167(2):425-430.
15. Nishimura T, Yamada N, Itoh A, Miyatake K. Cine MR imaging in mitral regurgitation: comparison with color Doppler flow imaging. Am J Roentgenol 1989;153(4):721-724.
16. Suzuki J, Caputo GR, Kondo C, Higgins CB. Cine MR imaging of valvular heart disease: display and imaging parameters affect the size of the signal void caused by valvular regurgitation. American Journal of Roentgenology 1990;155(4):723-727.
17. Mathieu J, Scott J. An Introduction to Turbulent Flow. Cambridge: Cambridge University Press; 2000.
18. Kuethe DO. Measuring distributions of diffusivity in turbulent fluids with magnetic-resonance imaging. Physical Review A 1989;40(8):4542-4551.
19. Gao JH, Gore JC. Turbulent flow effects on NMR imaging: measurement of turbulent intensity. Medical Physics 1991;18(5):1045-1051.
20. Gatenby JC, Gore JC. Mapping of turbulent intensity by magnetic resonance imaging. Journal of Magnetic Resonance B 1994;104(2):119-126.
21. Dyverfeldt P, Sigfridsson A, Kvitting JPE, Ebbers T. Quantification of intravoxel velocity standard deviation and turbulence intensity by generalizing phase-contrast MRI. Magn Reson Med 2006;56(4):850-858. [Erratum in: Magn Reson Med 2007;57(1):233]
22. Dyverfeldt P, Gårdhagen R, Sigfridsson A, Karlsson M, Ebbers T. On MRI Turbulence Quantification. Magn Reson Imaging 2009;27(7):913-922.
23. Elkins CJ, Alley MT, Saetran L, Eaton JK. Three-dimensional magnetic resonance velocimetry measurements of turbulence quantities in complex flow. Experiments in Fluids 2009;46(2):285-296.

24. Dyverfeldt P, Kvitting JPE, Sigfridsson A, Engvall J, Bolger AF, Ebbers T. Assessment of Fluctuating Velocities in Disturbed Cardiovascular Blood Flow: In-Vivo Feasibility of Generalized Phase-Contrast MRI. J Magn Reson Imaging 2008;28(3):655-663.
25. Ebbers T, Haraldsson H, Dyverfeldt P, Sigfridsson A, Warntjes M, Wigström L. Higher order weighted least-squares phase offset correction for improved accuracy in phase-contrast MRI. In: Proc 15th Int'l Soc Magn Reson Med; Berlin, Germany; 2007. p 1367.
26. Bryant DJ, Payne JA, Firmin DN, Longmore DB. Measurement of flow with NMR imaging using a gradient pulse and phase difference technique. Journal of computer assisted tomography 1984;8(4):588-593.
27. Heiberg E, Sjögren J, Ugander M, Carlsson M, Engblom H, Arheden H. Design and validation of Segment-freely available software for cardiovascular image analysis. BMC Medical Imaging 2010;10(1):1.
28. Klein AL, Bailey AS, Cohen GI, Stewart WJ, Duffy CI, Pearce GL, Salcedo EE. Importance of sampling both pulmonary veins in grading mitral regurgitation by transesophageal echocardiography. Journal of the American Society of Echocardiography 1993;6(2):115-123.
29. Buchner S, Debl K, Poschenrieder F, Feuerbach S, Riegger GAJ, Luchner A, Djavidani B. Cardiovascular Magnetic Resonance for Direct Assessment of Anatomic Regurgitant Orifice in Mitral Regurgitation. Circulation: Cardiovascular Imaging 2008;1(2):148-155.
30. Debl K, Djavidani B, Buchner S, Heinicke N, Fredersdorf S, Haimerl J, Poschenrieder F, Feuerbach S, Riegger GAJ, Luchner A. Assessment of the anatomic regurgitant orifice in aortic regurgitation: a clinical magnetic resonance imaging study. British Medical Journal 2008;94(3):e8.
31. Enriquez-Sarano M, Seward J, Bailey K, Tajik A. Effective regurgitant orifice area: a noninvasive Doppler development of an old hemodynamic concept. Journal of the American College of Cardiology 1994;23(2):443-451.
32. Enriquez-Sarano M, Avierinos J, Messika-Zeitoun D, Detaint D, Capps M, Nkomo V, Scott C, Schaff H, Tajik A. Quantitative determinants of the outcome of asymptomatic mitral regurgitation. The New England journal of medicine 2005;352(9):875-883.
33. Klein AL, Stewart WJ, Bartlett J, Cohen GI, Kahan F, Pearce G, Husbands K, Bailey AS, Salcedo EE, Cosgrove DM. Effects of mitral regurgitation on pulmonary venous flow and

left atrial pressure: An intraoperative transesophageal echocardiographic study. Journal of the American College of Cardiology 1992;20(6):1345-1352.

34. Passafini A, Shiota T, Depp M, Paik J, Ge S, Shandas R, Sahn DJ. Factors influencing pulmonary venous flow velocity patterns in mitral regurgitation: an in vitro study. Journal of the American College of Cardiology 1995;26(5):1333-1339.

35. Enriquez-Sarano M, Dujardin KS, Tribouilloy CM, Seward JB, Yoganathan AP, Bailey KR, Tajik AJ. Determinants of pulmonary venous flow reversal in mitral regurgitation and its usefulness in determining the severity of regurgitation. The American journal of cardiology 1999;83(4):535-541.

36. De Marchi S, Bodenmuller M, Lai D, Seiler C. Pulmonary venous flow velocity patterns in 404 individuals without cardiovascular disease. British Medical Journal 2001;85(1):23-29.

LIST OF TABLES

Table 1. Demographics and clinical data obtained by echocardiography

Subject	Sex	Age	Heart rate [min^{-1}]	Blood pressure [mmHg] [a]	LA diameter [mm] [b]	LV diameter [mm] [c]	Ejection fraction [%]	Peak jet velocity [m/s]
N1	M	57	71	N/A	37	49	60	-
N2	F	61	57	N/A	40	40	60	-
Pat1	M	66	47	130/70	50	58	55	6
Pat2	F	76	70	160/80	43	45	65	5
Pat3	M	41	57	140/90	45	62	65	5
Pat4	F	66	77	135/75	50	60	65	6
Pat5	F	57	61	155/95	45	61	60	6

N: normal subject, Pat: patient, LA: left atrium, LV: left ventricle

[a] systolic/diastolic blood pressure before the MRI scan

[b] LA anterior-posterior diameter at mid-systole

[c] LV anterior-posterior diameter at end diastole

Table 2. Intraoperative details of mitral valve morphology

Patient	Intraoperative findings
1	Prolapse of a discrete portion of the middle scallop of the PML due to chordal rupture.
2	Prolapse of the entire middle scallop of the PML due to chordal rupture and elongation.
3	Prolapse of a large part of the middle scallop of the PML with two chordal ruptures.
4	Prolapse of the entire middle scallop of the PML with multiple chordal ruptures.
5	Prolapse of a major part of the middle scallop and adjacent parts of the anterolateral and posteromedial scallops of the PML.

PML: Posterior mitral leaflet

LIST OF FIGURE LEGENDS

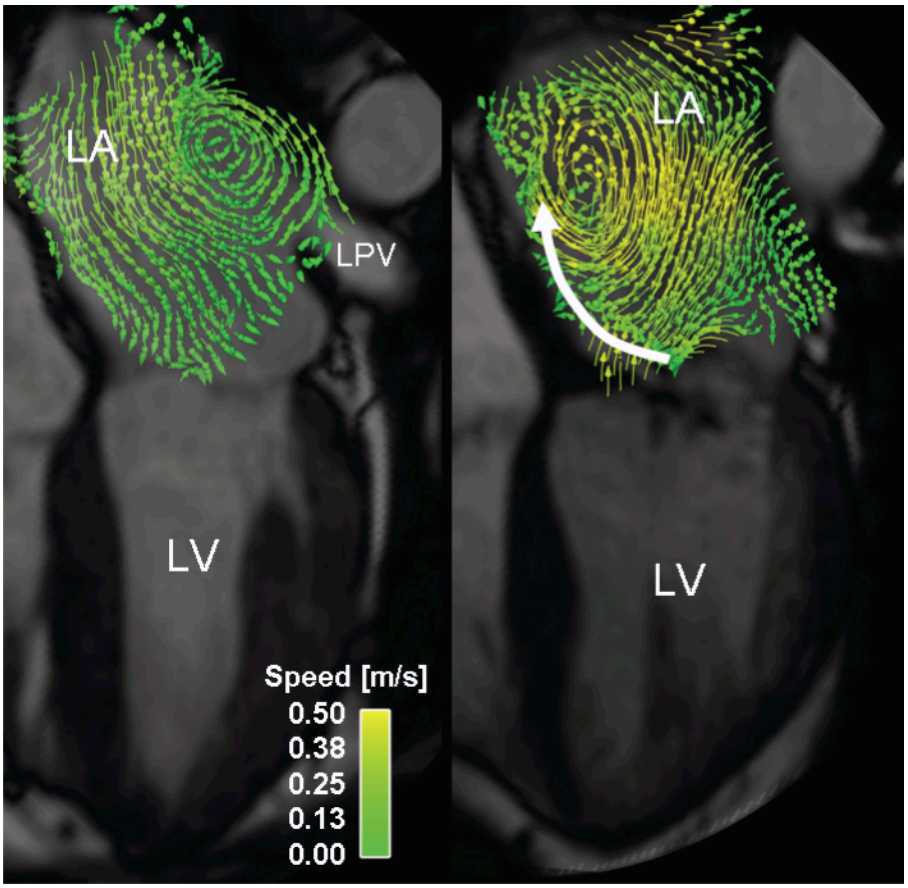

Figure 1. Visualization of left atrial (LA) flow patterns at peak systole in a normal subject (left) and a patient with an eccentric regurgitant jet directed towards the atrial septum (right). Pathlines were emitted from a plane in the LA and traced for 60 ms over peak systole; the colorbars indicate their speed. For anatomical orientation, a semi-transparent bSSFP 4-chamber image is provided (grayscale). In the normal subject, a counter-clockwise vortical flow is seen at the site of the inflow from the left pulmonary veins (LPV). In the patient, a pronounced vortical flow with clockwise rotation is seen at the septal side of the LA in proximity to the regurgitant jet. The regurgitant jet is indicated by the white arrow and is not apparent in the pathline visualization because of aliasing and the fact that it was located mainly outside of the emitter plane used. LV = left ventricle.

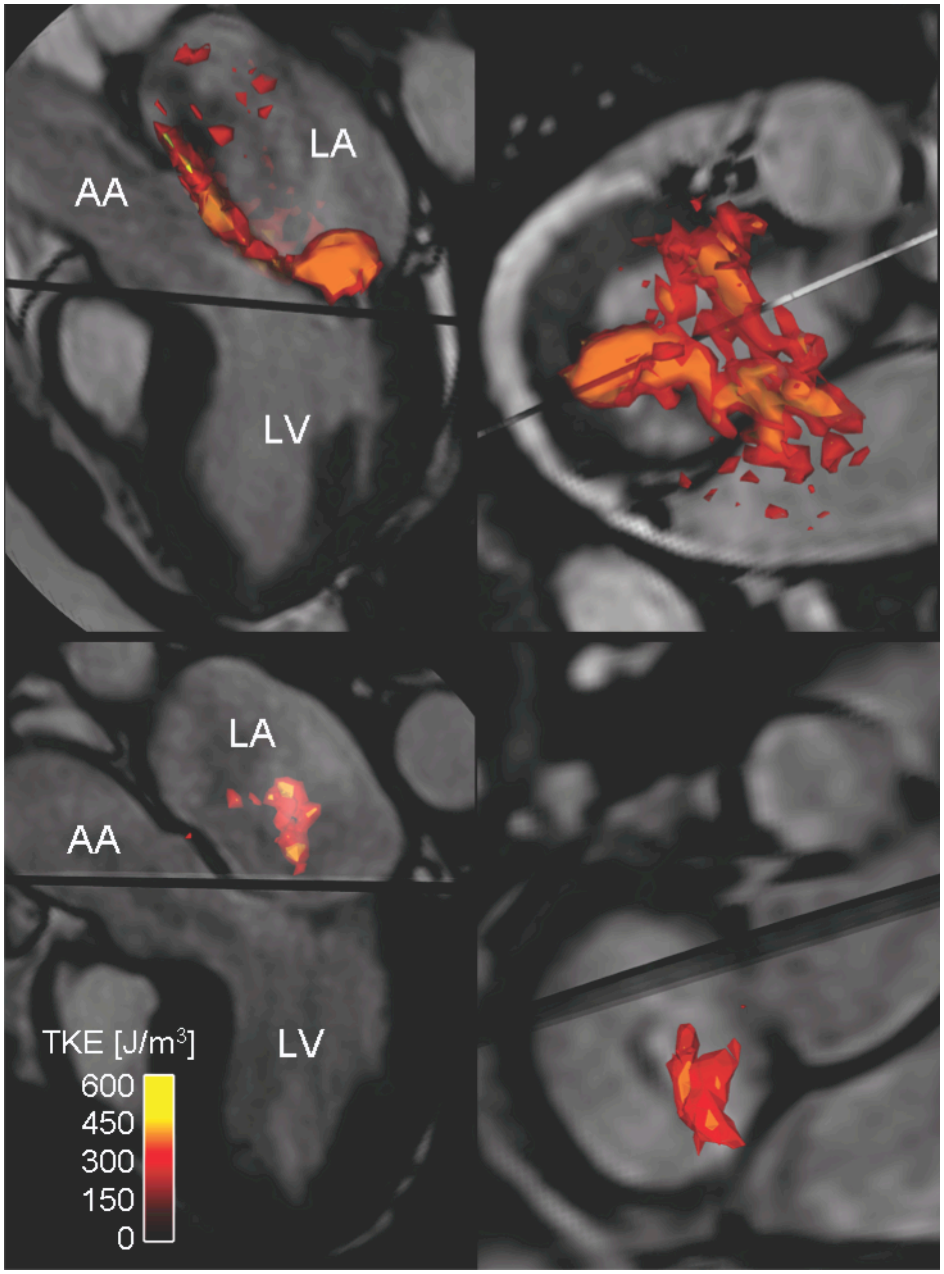

Figure 2. Left atrial (LA) flow with elevated turbulence intensity associated with mitral regurgitation. Visualization of turbulent kinetic energy (TKE) at late systole in a patient with an eccentric regurgitant jet (upper row) and a patient with a central jet (lower row). Iso-surfaces color coded according to TKE are shown in combination with semi-transparent morphological images in a 3-chamber view (left) and a short-axis view seen from base to apex (right). LV: left ventricle, AA: ascending aorta. The data shown in the upper row is typical for all the patients with eccentric jets directed towards the interatrial septum, where flow with high TKE is distributed over the septum.

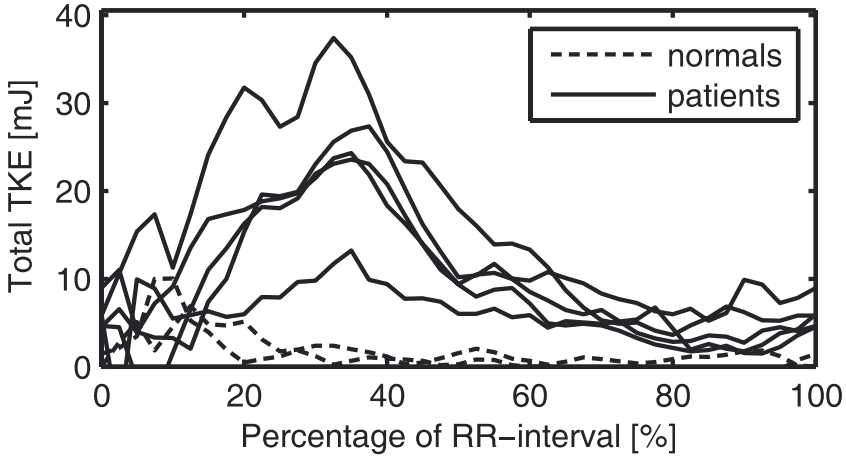

Figure 3. Temporal evolution of the total turbulent kinetic energy (TKE) in the left atrium. In the normal subjects (dashed lines), the TKE is low throughout the cardiac cycle. The mitral regurgitant patients (solid lines) demonstrate marked increases in TKE, with peak values occurring in late systole. The horizontal axis indicates the time in the cardiac cycle, expressed as the percentage of the RR-interval. Ventricular systole comprises the initial 35-40% of the cardiac cycle.

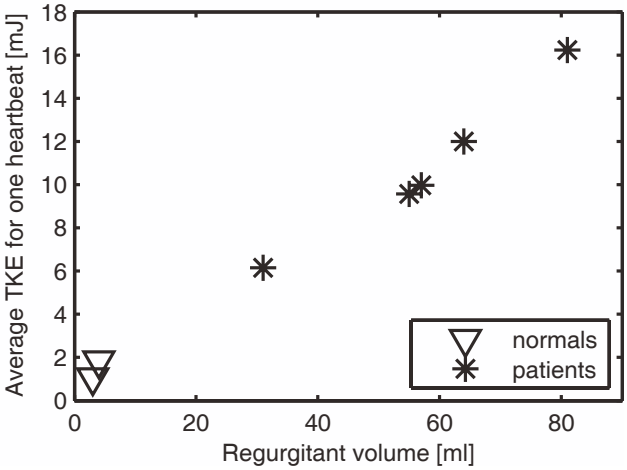

Figure 4. The average turbulent kinetic energy (TKE) in the left atrium per cardiac cycle plotted against the regurgitant volume for each subject. The average TKE was obtained by taking the sum of the total TKE for all time frames in one cardiac cycle and dividing by the number of time frames.

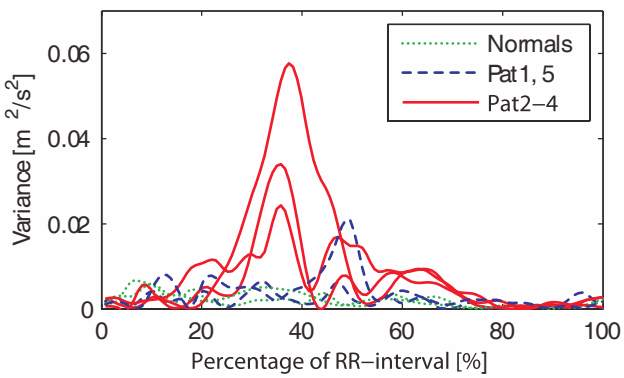

Figure 5. Discordances between the velocities in the pulmonary veins in normal subjects and patients (Pat) with mitral regurgitation. For each subject, the variance of the velocities between the pulmonary veins is plotted over one cardiac cycle. In three of the patients (Pat2-4) pronounced discordances are observed in late systole/early diastole (solid lines). In the normal subjects (solid lines with markers) as well as in the patients with the smallest and largest regurgitant volume (Pat1, Pat5) (dashed lines), respectively, this phenomenon was not observed. The horizontal axis indicates the time in the cardiac cycle, expressed as the percentage of the RR-interval. Ventricular systole comprises the initial 35-40% of the cardiac cycle.

MOVIE LEGENDS

Movie 1. Intraatrial flow with elevated turbulent kinetic energy (TKE) in a patient with an eccentric mitral regurgitant jet. Isosurfaces color coded according to TKE are shown in combination with semi-transparent morphological images in a 3-chamber view (main window) and a short-axis view seen from base to apex (small window). The upper plot shows the flow speed at the left ventricular outflow tract. The lower plot shows the total TKE in the left atrium over time. The TKE was obtained from a three-directional three-dimensional cine phase-contrast MRI measurement of the intravoxel velocity standard deviation (IVSD).